Mass Spectrometric Identification of Water-Soluble Gold Nanocluster Fractions from Sequential Size-Selective Precipitation

ARTICLE *in* ANALYTICAL CHEMISTRY · FEBRUARY 2012

Impact Factor: 5.64 · DOI: 10.1021/ac2029908 · Source: PubMed

4 AUTHORS, INCLUDING:

Xiupei Yang
China West Normal University
28 PUBLICATIONS **407** CITATIONS

analytical chemistry

Technical Note

pubs.acs.org/ac

Mass Spectrometric Identification of Water-Soluble Gold Nanocluster Fractions from Sequential Size-Selective Precipitation

Xiupei Yang,*[,†,§] Yan Su,[†] Man Chin Paau,[‡] and Martin M. F. Choi*[,‡]

[†]College of Chemistry and Chemical Engineering, China West Normal University, Nanchong 637000, P. R. China

[‡]Department of Chemistry, Hong Kong Baptist University, 224 Waterloo Road, Kowloon Tong, Hong Kong SAR, P. R. China

Supporting Information

ABSTRACT: This paper presents a simple and convenient methodology to separate and characterize water-soluble gold nanocluster stabilized with penicillamine ligands (AuNC-SR) in aqueous medium by sequential size-selective precipitation (SSSP) and mass spectrometry (MS). The highly polydisperse crude AuNC-SR product with an average core diameter of 2.1 nm was initially synthesized by a one-phase solution method. AuNCs were then precipitated and separated successively from larger to smaller ones by progressively increasing the concentration of acetone in the aqueous AuNCs solution. The SSSP fractions were analyzed by UV−vis spectroscopy, matrix-assisted laser desorption/ionization time-of-flight-MS, and thermogravimetric analysis (TGA). The MS and TGA data confirmed that the fractions precipitated from 36, 54, 72, and 90% v/v acetone ($F_{36\%}$, $F_{54\%}$, $F_{72\%}$, and $F_{90\%}$) comprised families of close core size AuNCs with average molecular formulas of $Au_{38}(SR)_{18}$, $Au_{28}(SR)_{15}$, $Au_{18}(SR)_{12}$, and $Au_{11}(SR)_8$, respectively. In addition, $F_{36\%}$, $F_{54\%}$, $F_{72\%}$, and $F_{90\%}$ contained also the typical magic-sized gold nanoparticles of Au_{38}, Au_{25}, Au_{18}, and Au_{11}, respectively, together with some other AuNCs. This study shed light on the potential use of SSSP for simple and large-scale preliminary separation of polydisperse water-soluble AuNCs into different fractions with a relatively narrower size distribution.

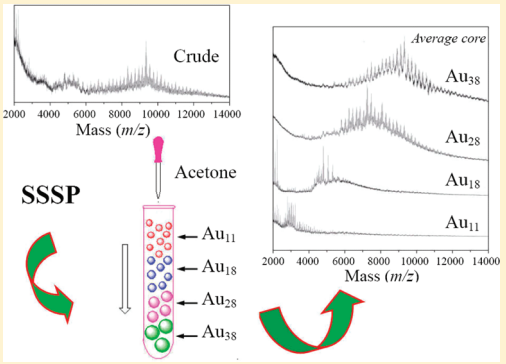

In recent years, nanoparticles (NPs), especially with subnanometer-sized metal cores, have attracted considerable attention because of their vast technological applications in catalysis, chemical recognition, magnetic materials, microelectronics, and optics. Monolayer protected nanoclusters (NCs) are subnanometer-sized (<~1 nm) metal crystallites which are stabilized by a covalently attached shell of ligands. Gold nanoparticles (AuNPs) protected from metal−metal aggregation by monolayers of thiolate ligands have aroused special interest because of the ease of manipulating the monolayer chemistry. Owing to the extraordinary stability of the thiolate-capped AuNCs, they have facilitated a broad range of fundamental and applied studies in recent years. Potential applications of AuNCs are currently being explored in many different areas. An important and challenging fact is that the as-synthesized small-sized AuNPs (1−5 nm core diameters) is generally a mixture of particles with different core sizes (i.e., polydispersity), and each NC/NP may have varying number of protecting ligands. This is especially true when a high degree of purity and monodispersity is desirable as they can affect their structure−function behavior, electronic properties, and optical properties or impede their self-assemble nanoscale structures.[1] Although a number of syntheses of AuNPs have been developed for NPs of varying core dimension and surface functionality,[2] the NP products still contain some impurities such as excess ligand, disulfide, salt, and starting material[3] and with a wide size range.[4] Variation of the initial reactant thiol-to-metal ratio and the temperature of the synthesis reaction has to a certain extent controlled the size and dispersity of NPs. Other methods including heating,[5] etching,[6] and annealing[7] have yielded specific monodisperse NP products but have not yet achieved a wide range of size control of monodisperse NPs. As such, there remains a challenge to develop strategies for the preparation of low disperse NPs with a control size range.[8]

Up until now, the separation and characterization of NPs are still attracting considerable interests. A variety of isolation techniques have been developed to narrow down the size distributions of NPs including solvent fractionation,[9] sedimentation/asymmetric-flow field flow fractionation,[10] centrifugation,[11] stirred-cell ultrafiltration,[12] diafiltration,[3c] gas expanded liquid extraction,[13] gel electrophoresis and/or capillary electrophoretic separation,[14] magnetic purification,[15] supercritical fluid extraction,[16] (analytical) ultracentrifugation and organic density gradient elution,[17] and liquid chromatographic separation.[11,18] The size-selective precipitation method is a general, non-destructive, and scalable separation technique, adapted from cadmium sulfide and cadmium selenide quantum dots separation technology and has demonstrated its potential for sorting NPs according to their chemical, structural, and size differences.[19] However, most size-selective precipitation work

Received: July 24, 2011
Accepted: January 9, 2012
Published: January 9, 2012

   dx.doi.org/10.1021/ac2029908 | *Anal. Chem.* 2012, 84, 1765−1771

focus on separating NPs from organic solvent,[20] and very few attempts are made to separate water-soluble functional NPs from aqueous media.[21] Although classical techniques for characterizing metal NP include scanning electron microscopy, transmission electron microscopy (TEM), and powder X-ray diffraction are widely used, these methods cannot directly discern the amount or size of the capping agent. Alternatively, mass spectrometry (MS) have emerged as a powerful tool for characterizing various types of nanomaterials. Electrospray ionization (ESI) MS has been successfully performed to characterize and determine the compositions of the metal core and ligand monolayer of small AuNPs.[22] So far Murray,[9c,23] Kornberg,[14o] Schaaff,[24] Dass,[25] Marsh,[26] and McLean and Cliffel[27] et al. have shown that laser desorption/ionization-MS, matrix-assisted laser desorption/ionization (MALDI)-MS, fast atom bombardment-MS, and MALDI-ion mobility-MS are not only effective approaches for NC/NP core size determination but can also assist to track the progress of fractionation/precipitation of AuNCs.

In this work, we present a convenient and efficient approach of sequential size-selective precipitation (SSSP) to purify and presize fractionate penicillamine-stabilized gold nanoclusters (AuNC-SR) in aqueous medium. The major advantage of SSSP is to use simple solvent systems to progressively fractionate a family of close core size AuNCs. The proposed methodology requires only readily available solvents for separation of AuNCs. This method shows considerable potential for efficient and convenient purification and high throughput size separation of water-soluble NC/NPs. SSSP offers a simple, clean, and tunable medium for dispersing metal particles. The particle size range can be controlled by simply varying the concentration of organic solvent used for precipitation. Since MALDI-MS has emerged as an indispensable tool in accurate assessment of the core size of NPs, it is employed to identify the major mass components of each SSSP fraction. In addition, the UV−vis absorption spectra of each SSSP fraction are acquired to assess their changes in size distribution. Finally, thermogravimetric analysis (TGA) is used to determine the amounts of ligand attached to the AuNCs of the SSSP fractions. The AuNCs in the crude product and SSSP fractions have been successfully characterized by the UV−vis, MS, and TGA methods.

EXPERIMENTAL SECTION

Chemicals. Hydrogen tetrachloroaurate(III) trihydrate ($HAuCl_4{\cdot}3H_2O$, 99.9%), D-penicillamine (99%), and sodium borohydride ($NaBH_4$) (99%) were purchased from Aldrich (Milwaukee, WI). 2,5-Dihydroxybenzoic acid (DHB, 98%) was obtained from Sigma (St. Louis, MO). HPLC-grade ethanol (EtOH) and methanol (MeOH) and AR-grade acetone (>99.99%) were from Labscan (Bangkok, Thailand). Glacial acetic acid was purchased from Beijing Chemical Plant (Beijing, China). Concentrated hydrochloric acid was from Farco Chemical Supplies (Beijing, China). Purified water from a Milli-Q-RO4 water purification system (Millipore, Bedford, MA) with a resistivity higher than 18 MΩ cm was used to prepare all solutions. All reagents of analytical grade or above were used as received.

UV−Visible Absorption Spectroscopy. The UV−vis absorption spectra of the SSSP fractions in water were recorded on a Cary 100 Scan UV−vis absorption spectrophotometer (Varian, Palo Alto, CA) over the wavelength range from 250 to 800 nm. The spectra were normalized at 250 nm to remove the effect of concentration difference.

Matrix-Assisted Laser Desorption Ionization-Mass Spectrometry. The SSSP fractions were analyzed by a MALDI time-of-flight (TOF) MS (Autoflex, Bruker, Germany). The SSSP fraction was mixed (1:1 v/v) with a 1.0 M solution of DHB in $MeOH/H_2O$ (1:1 v/v). Then 4.0 μL of this solution was deposited on a MALDI target plate and air-dried. The sample was inserted into the instrument and irradiated by a pulsed nitrogen (N_2) laser working at 337 nm. In general, 30 laser shots were averaged for each spectrum. The mass accuracy for the investigated scan range was 100 ppm, i.e., ±1−2 mass units.

Thermogravimetric Analysis. TGA was acquired on a Perkin-Elmer TGA 6 thermogravimetric analyzer (Waltham, MA). About 5 mg of SSSP fraction sample was put into a ceramic pan and the temperature was ramped from 50 to 400 °C at a heating rate of 10 °C/min.

RESULTS AND DISCUSSION

Synthesis and Sequential Size-Selective Precipitation of the Crude Nanoclusters. Penicillamine-stabilized AuNCs were prepared using procedures as described previously[14e,j,k] with some minor modifications. Briefly, 0.592 g (1.50 mmol) of $HAuCl_4{\cdot}3H_2O$ and 0.672 g (4.50 mmol) of D-penicillamine were codissolved in 30 mL of MeOH/glacial acetic acid (6:1 v/v) at 0 °C. After about 30 s stirring, the reaction mixture changed from bright yellow to orange with some white suspensions. The mixture was reduced immediately on addition of 3.0 mL of 1.135 g (30.0 mmol) $NaBH_4$ in EtOH and the solution became dark brown. After further stirring for 30 min, the reaction mixture was precipitated by adding 60 mL of acetone. Most solvents were then removed by centrifugation and evaporation. The dark brown crude AuNC product was redissolved in ∼0.2 mL of H_2O and adjusted to pH ∼1 by dropwise addition of concentrated HCl to protonate the carboxylate moieties of the protected ligands. Then the AuNCs were precipitated by adding 60 mL of acetone. After the removal of solvent, the residues were resuspended in 60 mL of acetone and centrifuged. The dark brown product was removed from the centrifugation tube and dried under a stream of N_2 at ambient conditions. The spherical polydisperse penicillamine-stabilized AuNC product, with confirmed average core size of 2.1 nm by HRTEM (Figure S1 of the Supporting Information), was designated as the crude AuNC product.

SSSP was applied to separate the crude AuNC product into different AuNC fractions of various core sizes as shown in the scheme in Figure 1. Fractionations were performed by incrementally adding an organic solvent (in here, acetone) to sequentially precipitate AuNCs in aqueous medium from the larger to the smaller sizes. A typical procedure started with 150 mg of the as-synthesized AuNCs in 10 mL of H_2O. A known volume of acetone was added to the aqueous AuNCs solution so that the acetone volume percentage in the total solution was 36% and some of the AuNCs were then precipitated. After standing for 30 min, the mixture was separated by a centrifuge (D-78532, Hettich Zentrifugen, Tuttlingen, Germany) at 6000 rpm for 10 min to obtain the precipitate and supernatant layer. The precipitate was collected and dried in a stream of N_2 at ambient conditions which was designated as the $F_{36\%}$ fraction. The supernatant layer was transferred to another tube and more acetone was added so that its volume percentage in the total solution was 54% to induce the precipitation of another fraction of AuNCs ($F_{54\%}$). Separation of $F_{54\%}$ from the supernatant was again succeeded by centrifugation. This SSSP

dx.doi.org/10.1021/ac2029908 | Anal. Chem. 2012, 84, 1765−1771

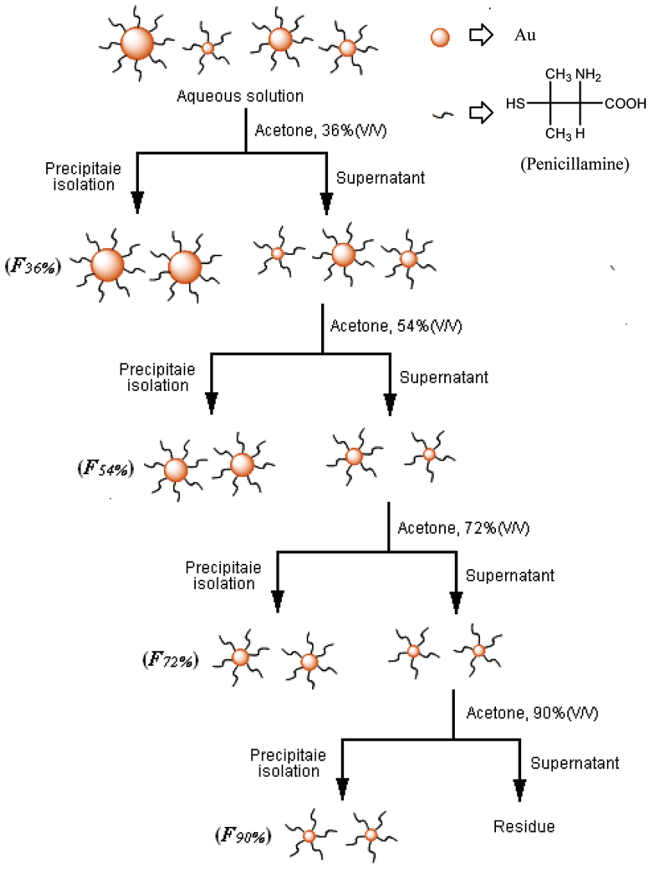

Figure 1. Schematic diagram of sequential size-selective precipitation (SSSP) of an AuNC mixture.

process was repeated two more times by adding more acetone to the supernatant to collect fractions of AuNCs as $F_{72\%}$ and $F_{90\%}$, respectively. Finally, the remaining supernatant was collected and dried in a stream of N_2 at ambient conditions which was designated as residue.

Infrared Spectroscopic Analysis. Since the ligand (penicillamine shown in Figure 1) contains both the thiol and amine moieties, theoretically both can protect the AuNCs. In order to assess this competition binding, the infrared (IR) spectra of the penicillamine-stabilized AuNCs and the free ligand were taken and shown in Figure S2 in the Supporting Information. The absorption bands at 3440, 2960, and 1700 cm^{-1} are attributed to the stretching vibration of −OH, $-CH_3$, and −C═O of the free ligand, respectively. The bands at 3100 and 2560 cm^{-1} are assigned to the $-NH_2$ and −SH groups in the free ligand. Comparing the IR spectrum of penicillamine-stabilized AuNCs with the free penicillamine ligand, the corresponding bands at 3440, 3100, 2960, and 1700 cm^{-1} are slightly shifted due to the interaction of penicillamine with the surface of AuNCs. However, the absorption band at 3100 cm^{-1} corresponding to the $-NH_2$ moiety still remains for the penicillamine-stabilized AuNCs whereas the S−H stretching band at 2560 cm^{-1} completely disappears, inferring that our pencilliamine-stabilized AuNCs were mainly protected by the Au−S instead of the Au−N bond.

Optical Absorption Properties. Figure 2 depicts the UV−vis absorption spectra of the SSSP fractions. These spectra are normalized at 250 nm to remove the effect of concentration differences so as to focus on comparing their spectral shape and band position. Negishi et al.[14b,d] and our previous work[14j,18i]

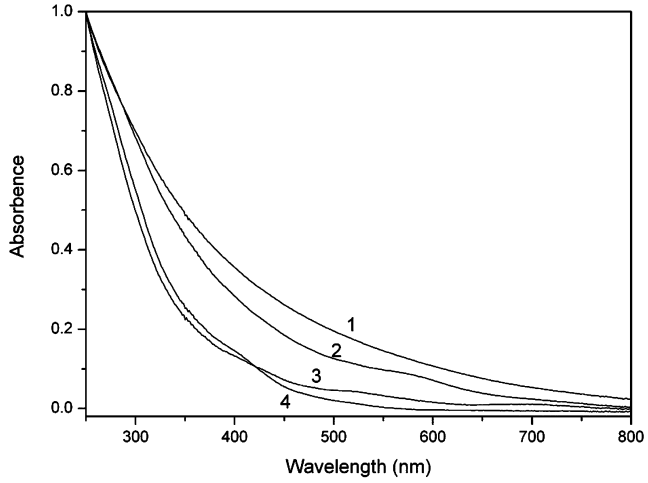

Figure 2. UV−visible absorption spectra of the SSSP fractions: (1) $F_{36\%}$, (2) $F_{54\%}$, (3) $F_{72\%}$, and (4) $F_{90\%}$.

observed that smaller core AuNCs possess a sharper decrease in absorbance than that of larger core AuNCs from shorter to longer wavelengths. In essence, large core AuNC produces an absorption spectrum with relatively higher absorbance than that of small core AuNC in the visible light region. For AuNCs with core diameter less than 3 nm, the surface plasmon (SP) band becomes broadened into the baseline and the absorption spectrum displays only a featureless exponential decay profile,[28] and for even smaller NCs (<2 nm), some molecular features may start to appear attributing to the emergence of a HOMO−LUMO bandgap.[29] Fractions $F_{72\%}$ and $F_{90\%}$ are more structural at <∼500 nm, indicating that they are very small, molecule-like AuNCs whereas fractions $F_{36\%}$ and $F_{54\%}$ are less pronounced, suggesting that each fraction possesses a family of close core size AuNCs. For the $F_{36\%}$ fraction, only a featureless absorption profile is observed which is identified by the MS to contain Au_{38} and close core size clusters (vide infra). For the $F_{54\%}$ fraction, a better-defined absorption shoulder peak at 575 nm emerges and is designated to contain Au_{25}, Au_{28}, and other close core size clusters by MS (vide infra). For the $F_{72\%}$ fraction, three well-defined absorption maximum and shoulder peaks at 418, 513, and 692 nm are located, which are the typical characteristic absorption features of Au_{18} clusters. The first two absorption bands are ascribed to the NC interband electronic transitions and the third one to the excitonic transition of the semiconductor-like HOMO−LUMO bandgap of the subnanometer-sized clusters.[30] For the $F_{90\%}$ fraction comprising mainly Au_{11} clusters, its absorption spectrum with a shoulder peak at 410 nm decays in an approximately exponential fashion from the UV to visible regions with no detectable SP band. The spectral characteristics of our small and large core AuNCs are in complete agreement with the previous AuNCs.[14e] The differences in the normalized absorption spectra of the four SSSP fractions well demonstrate that the particle size of AuNCs obtained from the SSSP fractionation follows in the trend: $F_{36\%} > F_{54\%} > F_{72\%} > F_{90\%}$. All these absorption spectra indicate that the size of AuNCs spontaneously narrows down over the SSSP process although the molecularly monodisperse AuNCs are not obtained.

Mass Spectrometric Studies of Sequential Size-Selective Precipitation Fractions. MALDI-MS was applied to characterize the crude and the four SSSP fractions of penicillamine-stabilized AuNCs. The crude AuNC product was

dx.doi.org/10.1021/ac2029908 | Anal. Chem. 2012, 84, 1765−1771

quite polydisperse as revealed by MS (*vide infra*) and HRTEM (Figure S1 in the Supporting Information). The MALDI-MS of the crude AuNC product (A) and the fractions $F_{36\%}$, $F_{54\%}$, $F_{72\%}$, and $F_{90\%}$ (parts B, C, D, and E, respectively) are displayed in Figure 3. The MS of the as-prepared penicillamine-stabilized

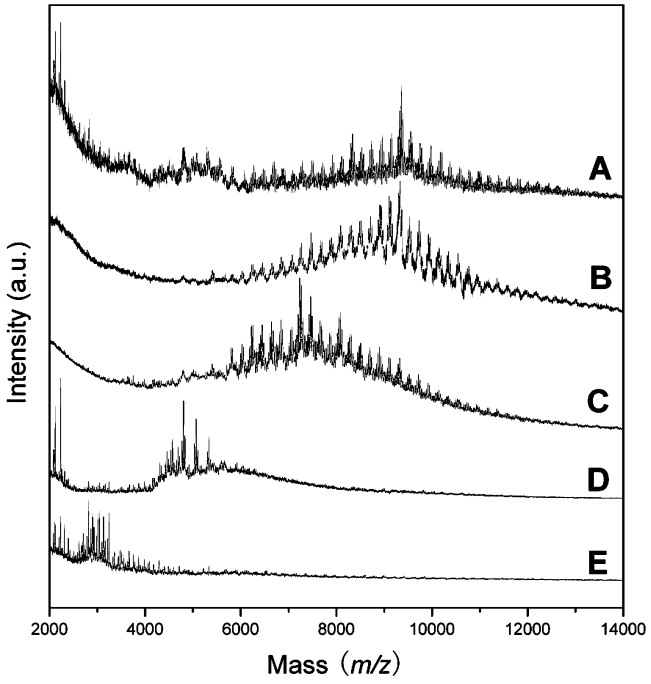

Figure 3. MALDI-TOF mass spectra of the crude penicillamine-stabilized AuNC product (A) and the SSSP fractions: (B) $F_{36\%}$, (C) $F_{54\%}$, (D) $F_{72\%}$, and (E) $F_{90\%}$.

AuNC product (Figure 3A) displays a relatively smooth distribution of mass peaks ranging 2.0−14 kDa with three major humps at ∼3.8, 5.0, and 9.3 kDa. Spectra taken at lower laser fluence did not lead to the convergence of the peaks into one major peak, suggesting that these major peaks were not originated from the fragmentation of a single size AuNC; instead they should correspond to AuNCs of different sizes. These results concur with the MS analysis of the SSSP fractions as depicted in Figure 3B−E. It is clearly seen that the MS show a reduction in dispersity of AuNCs as the SSSP fractionation proceeds with the increase in acetone content in the aqueous medium. The major mass peaks of $F_{36\%}$, $F_{54\%}$, $F_{72\%}$, and $F_{90\%}$ center at ∼9330, 7280, 4800, and 3250 Da, respectively, inferring that the SSSP fraction decreases in mass with the increase in acetone content. The MS confirm that the larger AuNCs are precipitated first at low acetone content, followed with the smaller AuNCs and then finally the smallest with the progressive increase in acetone content in the aqueous medium. Figure S3 in the Supporting Information displays clearer MS for all the SSSP fractions after baseline subtraction. We have attempted to optimize the matrix and laser power in the MALDI-MS experiments but it is very difficult to obtain a single parent ion for each fraction. Thus, our MS of each fraction could only provide an estimation of the main and some minor components of the AuNC sample.

Figure 4 depicts the expanded MS of the SSSP fraction $F_{36\%}$ with a main peak centered at 9338 Da corresponding to the $[Au_{35}(SR)_{15}S_7]$ fragment which is derived from the loss of three Au atoms, two ligands (SR), and carbon chain moieties of the

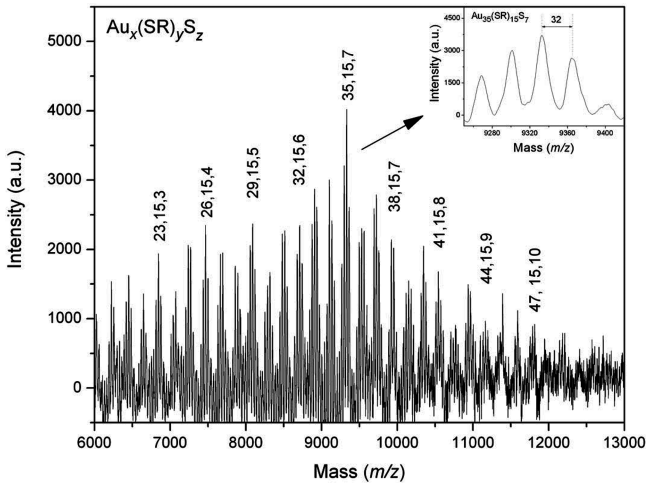

Figure 4. Expanded MALDI-TOF mass spectrum of the SSSP fraction $F_{36\%}$ in the mass range 6 000−13 000 Da. The mass spectrum was baseline corrected by using the FlexAnalysis software. The mass peaks are assigned to $Au_x(SR)_yS_z$ and denoted as *x*, *y*, *z*, where *x*, *y*, and *z* are the numbers of Au atoms, intact penicillamine ligands, and S atoms, respectively. The inset displays the close-up view of the mass spectrum of the $[Au_{35}(SR)_{15}S_7]$ species. The spacing between the isotopic peak is 32, corresponding to the relative atomic mass of S.

$Au_{38}(SR)_{24}$ clusters since Au_{38} is the well-established and identified NC species.[31] The low-mass and high-mass sides of the 9338 *m*/*z* peak show a series of fragments and recombined ion peaks in the clusters of this fraction. There are other $Au_x(SR)_yS_z$ mass peaks, inferring that the $F_{36\%}$ fraction could also contain other NCs close to Au_{38}. When cluster compounds are irradiated, the ions detected can be described as major and minor *m*/*z* spacings which are consistent with the original composition of the cluster core. The peak labeled as *x*, *y*, and *z* represent the numbers of Au atoms, intact penicillamine ligands (SR), and S atoms (ligands by which C−S bond cleavage have lost their carbon portions), respectively. The series of peaks in Figure 4 are ascribed to the distinctive pattern of fragmentations. The detailed peak assignments of most mass peaks to the general $Au_x(SR)_yS_z$ formula are summarized in Table S1 (Supporting Information). All the peak assignments are within the mass accuracy (±1−2 mass units) of the MALDI-TOF MS. These series of peaks arise from the successive mass losses equivalent to one Au atom and/or with a sulfur loss, resulting in the major *m*/*z* spacing between the most abundant ion in each adjacent group corresponding to a mass difference of either 197 (Au) or 229 (AuS). The inset depicts the close-up view of the MS of the $[Au_{35}(SR)_{15}S_7]$ species in Figure 4. The repetitive spacing between the isotopic peaks is generally 32 Da, corresponding to the exact atomic weight of S. A similar fragmentation phenomenon has been observed by Murray and his co-workers.[23c] This minor spacing is also found in each group of ions in Figure 4.

Figures 5−7 display the expanded MS of the SSSP fraction $F_{54\%}$, $F_{72\%}$, and $F_{90\%}$ with the most abundant peaks at 7272, 4794, and 3235 *m*/*z*. The assignments of the series of peaks in Figures 5−7 are summarized in Tables S2−S4 in the Supporting Information. The "average" composition of these three fractions can be described as the $Au_{28}(SR)_{15}$, $Au_{18}(SR)_{12}$, and $Au_{11}(SR)_8$, respectively, with reference to the most abundant species and the TGA results shown in Figure 8 (vide infra). It should be borne in mind that the assigned

dx.doi.org/10.1021/ac2029908 | *Anal. Chem.* 2012, 84, 1765−1771

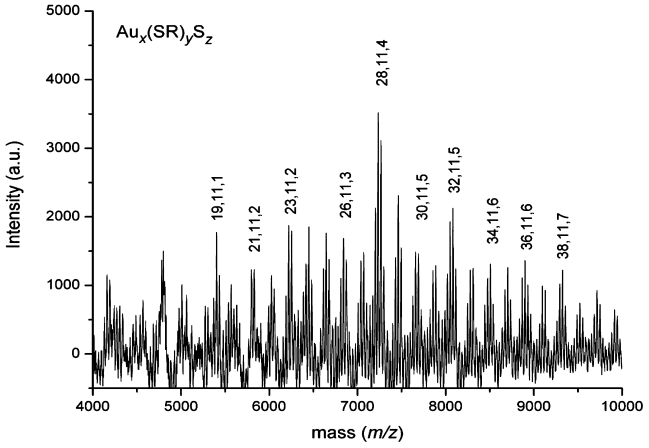

Figure 5. Expanded MALDI-TOF mass spectrum of the SSSP fraction $F_{54\%}$ in the mass range 4 000−10 000 Da. The mass spectrum was baseline corrected by using the FlexAnalysis software. The mass peaks are assigned to $Au_x(SR)_ySz$ and denoted as *x*, *y*, and *z*, where *x*, *y*, and *z* are the numbers of Au atoms, intact penicillamine ligands, and S atoms, respectively.

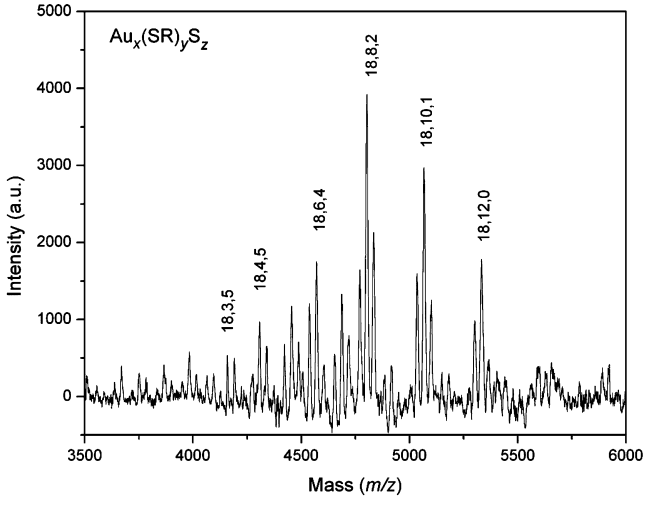

Figure 6. Expanded MALDI-TOF mass spectrum of the SSSP fraction $F_{72\%}$ in the mass range 3 500−6 000 Da. The mass spectrum was baseline corrected by using the FlexAnalysis software. The mass peaks are assigned to $Au_x(SR)_ySz$ and denoted as *x*, *y*, and *z*, where *x*, *y*, and *z* are the numbers of Au atoms, intact penicillamine ligands, and S atoms, respectively.

formula only represents an average value since each fraction comprises AuNCs of close core sizes. The formulas can be more accurate if each fraction is further purified by other analytical separation techniques such as capillary electrophoresis and high-performance liquid chromatography. Future work will be pursued in this direction.

It is interesting to note that the major *m*/*z* spacing between the most abundant ions in each adjacent group obtained from $F_{72\%}$ is not similar to that of the other three SSSP fractions. Figure 6 indicates that the MS does not contain *m*/*z* 197 (Au) or 229 (AuS) peaks as the other three fractions; instead, *m*/*z* 234 and 266 peaks are observed. This series of peaks arises from the successive mass losses equivalent to two penicillamine units plus (one or two) sulfur, i.e., loss of a carbon chain R_2 (*m*/*z* 234.28) or a sulfide SR_2 (*m*/*z* 266.35).[23c] The $[Au_{18}(SR)_{10}S]$ peak (*m*/*z* 5060.65) corresponds to the loss of

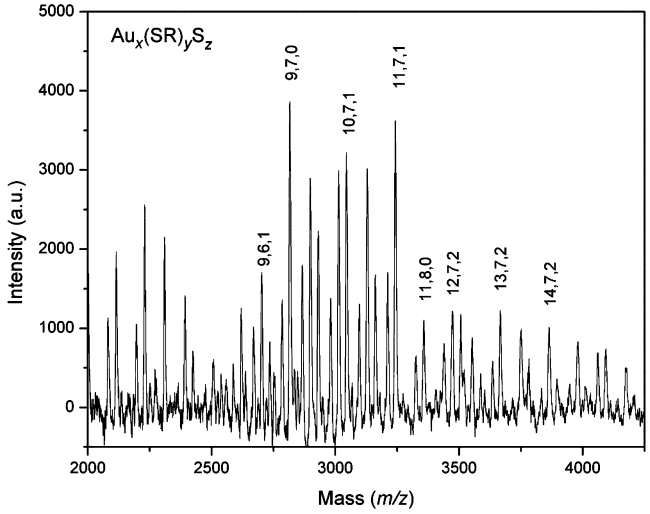

Figure 7. Expanded MALDI-TOF mass spectrum of the SSSP fraction $F_{90\%}$ in the mass range 2 000−4 250 Da. The mass spectrum was baseline corrected by using the FlexAnalysis software. The mass peaks are assigned to $Au_x(SR)_ySz$ and denoted as *x*, *y*, and *z*, where *x*, *y*, and *z* are the numbers of Au atoms, intact penicillamine ligands, and S atoms, respectively.

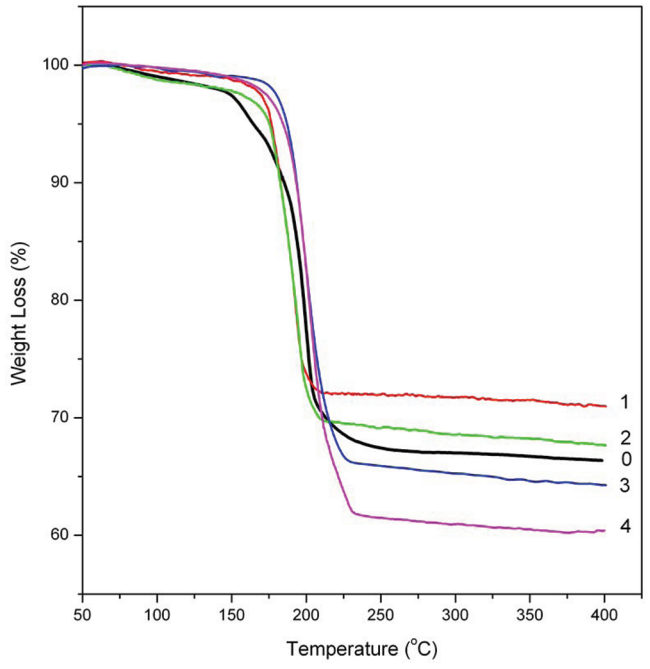

Figure 8. TGA analyses of the crude penicillamine-stabilized AuNC product (0) and the SSSP fractions: (1) $F_{36\%}$, (2) $F_{54\%}$, (3) $F_{72\%}$, and (4) $F_{90\%}$.

a SR_2 group from $Au_{18}(SR)_{12}$ (*m*/*z* 5324.94). These characteristic fragmentations of AuNCs are similar to previous results of $Au_{25}(SR)_{18}$ clusters.[25a,b] In addition, positive-ion ESI-MS was used to identify the composition of the unprecipitated fraction (residue) in 90% v/v acetone as depicted in Figure S4 in the Supporting Information. This fraction mainly contains the disulfide ligand S_2R_2 (*m*/*z* 296.9) which is derived from the reaction between $HAuCl_4$ and RSH (i.e., $HAuCl_4$ + 3RH → Au-SR + RS-SR + 4HCl) in the synthesis of AuNCs. This byproduct, fortunately, can be removed by the SSSP. Other minor byproduct such as S_2R (*m*/*z* 179.8) and S_4R_4 (*m*/*z*

dx.doi.org/10.1021/ac2029908 | *Anal. Chem.* 2012, 84, 1765−1771

593.3) are also observed, which are probably derived from the decomposition of the Au(I)-SR polymer in the process of AuNCs synthesis.

Figure 8 displays the TGA of the crude penicillamine-stabilized AuNC product and the SSSP fractions. The weight loss of the crude AuNC product, and SSSP fractions $F_{36\%}$, $F_{54\%}$, $F_{72\%}$, and $F_{90\%}$ are 31.11, 26.32, 29.26, 33.85, and 36.11 wt %, respectively. The XPS analysis (Figure S5 in the Supporting Information) confirms that the crude AuNC product consists of mainly Au atoms and protected ligands; thus, the four SSSP fractions should only contain Au atoms and thiolate ligands as well. The weight loss increases with the increase in acetone content for SSSP fractions, indicating that the ligand content in AuNC increases in the trend: $F_{36\%} < F_{54\%} < F_{72\%} < F_{90\%}$, corresponding to the Au/SR ratio of 2.11, 1.82, 1.47, and 1.33, respectively. The TGA results infer that the core size of AuNC in the SSSP fractions follows as $F_{36\%} > F_{54\%} > F_{72\%} > F_{90\%}$ since larger NPs usually have a smaller ligand mass fraction.[18i] In other words, $F_{36\%}$ contains AuNCs of the largest core sizes whereas $F_{90\%}$ has the smallest. These results are in complete agreement with our MS data (vide supra). The average molecular formulas of $Au_x(SR)_y$ for $F_{36\%}$, $F_{54\%}$, $F_{72\%}$, and $F_{90\%}$ are determined as $Au_{38}(SR)_{18}$, $Au_{28}(SR)_{15}$, $Au_{18}(SR)_{12}$, and $Au_{11}(SR)_8$, respectively, based on the TGA and MS results.

The MS results prove that our water-soluble AuNCs can be sequentially separated from an aqueous medium according to their core size by increasing the acetone content. It can be explained that the water solubility of AuNCs is mainly governed by particle size and the hydrophilic ligands on the Au core surface. In other words, the ligand/Au ratios of the SSSP fractions ($F_{36\%}$, $F_{54\%}$, $F_{72\%}$, and $F_{90\%}$) increase gradually, resulting in better water-solubility from $F_{36\%}$ to $F_{90\%}$. The charged and polar surface ligands interact with the water molecules, thus, increase water-solubility. Repulsive electrostatic forces between the NPs are formed when the water-soluble NPs are suspended in an aqueous solution. These repulsive forces can prevent NP aggregation and facilitate dissolution. The DLVO theory states that the magnitude of the energy barrier and maximum repulsive force is determined by the dielectric constant, surface potential, and particle size.[32] For pure aqueous solution, the dielectric constant of the solvent is high and the maximum repulsive force is high too. Under this condition, AuNCs are stable against aggregation. When acetone is added to the AuNC aqueous solution, the dielectric constant of the solvent decreases and so does the maximum repulsive force. As such, if the dielectric constant of the medium decreases with the addition of organic solvent, the solubility of AuNCs should decrease and precipitation should be expected. In addition, since the larger particles have stronger attraction forces, they are flocculated first whereas the smaller particles are still stabilized by the hydration layer. It is obvious that the larger the particle, the stronger the influence it exerts on adjacent particles and hence the stronger the interparticulate forces. In other words, the van der Waals forces increase with particle size; the larger the interactive particles, the stronger their interaction due to such forces. As the van der Waals forces are proportional to particle size, it is thus possible to collect the monodisperse size of the samples by controlling the amount of antisolvent added. In essence, this is why the SSSP technique can be applied successfully to fractionate water-soluble AuNCs of various core sizes.

CONCLUSIONS

In summary, we have demonstrated a convenient and efficient method to isolate and purify a polydisperse AuNC sample. Our experiments have shown that SSSP is particularly suitable for preliminary large-scale purification and fractionation of water-soluble AuNCs. The SSSP possesses flexibility of selecting the required family size of NPs by just adjusting the organic solvent fraction in the NP solution. Additionally, SSSP will be useful in producing bulk quantities of NPs with narrower size distribution for future applications. In here, four fractions of AuNCs with average Au_{11}, Au_{18}, Au_{28}, and Au_{38} cores could be separated from its original highly polydisperse AuNC product. The clusters of these fractions were successfully characterized by UV−vis spectroscopy, MS, and TGA. The higher purity and narrower size distribution of NPs afforded by SSSP will allow for more precise determination of their catalytic, electronic, and optical properties, easier assessment of their structure−function relationships in toxicology studies, and greater reproducibility in self-assembly of AuNCs. Finally, further optimization of SSSP should result in fractionation of AuNCs into specific sizes on the gram scale that may exhibit particular properties for specialized applications.

ASSOCIATED CONTENT

Supporting Information

Experimental procedures for HRTEM, XPS, and IR, supplementary figures of HRTEM, IR, MALDI-TOF MS of the crude penicillamine-stabilized AuNC product and SSSP fractions after baseline subtraction, positive-ion ESI-MS of the residue fraction and wide-scan XPS spectrum of the crude penicillamine-stabilized AuNC product, and tables of mass spectral assignments versus calculated mass. This material is available free of charge via the Internet at http://pubs.acs.org.

AUTHOR INFORMATION

Corresponding Author

*E-mail: xiupeiyang@163.com (X.Y.); mfchoi@hkbu.edu.hk (M.M.F.C.).

Notes

[§]Visiting Scholar to Hong Kong Baptist University.

ACKNOWLEDGMENTS

Financial support from the HKBU Faculty Research Grant (Project No. FRG2/08-09/077) is gratefully acknowledged. M. C. Paau acknowledges the receipt of a postgraduate studentship from the Additional UGC-funded Research Postgraduate Places in the area of Environmental and Human Health Risk Assessment of Persistent Toxic Substance. We would express our sincere thanks to Ms. Silva T. Mo of the Department of Chemistry, Hong Kong Baptist University for acquiring the MALDI-TOF MS data and Ms. Winnie Y. K. Wu of the Centre for Surface Analysis and Research, Hong Kong Baptist University for recording the HRTEM and XPS data of the AuNC sample. The HRTEM used in this work was supported by the Special Equipment Grant from the University Grants Committee of the Hong Kong Special Administrative Region, China (Grant SEG_HKBU06).

REFERENCES

(1) (a) Thomas, K. G.; Kamat, P. V. *Acc. Chem. Res.* **2003**, *36*, 888−898. (b) Foster, E. W.; Kearns, G. J.; Goto, S.; Hutchison, J. E. *Adv. Mater.* **2005**, *17*, 1542−1545. (c) Kearns, G. J.; Foster, E. W.;

Hutchison, J. E. *Anal. Chem.* **2006**, *78*, 298−303. (d) Eustis, S.; El-Sayed, M. A. *Chem. Soc. Rev.* **2006**, *35*, 209−217.
(2) (a) Weare, W. W.; Reed, S. M.; Warner, M. G.; Hutchison, J. E. *J. Am. Chem. Soc.* **2000**, *122*, 12890−12891. (b) Kanaras, A. G.; Kamounah, F. S.; Schaumburg, K.; Kiely, C. J.; Brust, M. *J. Chem Soc., Chem. Commun.* **2002**, 2294−2295.
(3) (a) Cumberland, S. L.; Berrettini, M. G.; Javier, A.; Strouse, G. F. *Chem. Mater.* **2003**, *15*, 1047−1056. (b) Wang, D.; He, J.; Rosenzweig, N.; Rosenzweig, Z. *Nano Lett.* **2004**, *4*, 409−413. (c) Sweeney, S. F.; Woehrie, G. H.; Hutchison, J. E. *J. Am. Chem. Soc.* **2006**, *128*, 3190−3197.
(4) Anand, M.; McLeod, M. C.; Bell, P. W.; Roberts, C. B. *J. Phys. Chem. B* **2005**, *109*, 22852−22859.
(5) Shimizu, T.; Teranishi, T.; Hasegawa, S.; Miyake, M. *J. Phys. Chem. B* **2003**, *107*, 2719−2724.
(6) Schaaff, T. G.; Whetten, R. L. *J. Phys. Chem. B* **1999**, *103*, 9394−9396.
(7) Hicks, J. F.; Miles, D. T.; Murray, R. W. *J. Am. Chem. Soc.* **2002**, *124*, 13322−13328.
(8) Zhang, Q.; Xie, J.; Yu, Y.; Lee, J. Y. *Nanoscale* **2010**, *2*, 1962−1975.
(9) (a) Schaaff, T. G.; Shafigullin, M. N.; Khoury, J. T.; Vezmar, I.; Whetten, R. L.; Cullen, W. G.; First, P. N.; Gutiérrez-Wing, C.; Ascensio, J.; Jose-Yacamán, M. J. *J. Phys. Chem. B* **1997**, *101*, 7885−7891. (b) Chen, S.; Murray, R. W. *J. Phys. Chem. B* **1999**, *103*, 9996−10000. (c) Hicks, J. F.; Templeton, A. C.; Chen, S.; Sheran, K. M.; Jasti, R.; Murray, R. W.; Debord, J.; Schaaff, T. G.; Whetten, R. L. *Anal. Chem.* **1999**, *71*, 3703−3711.
(10) (a) Calzolai, L.; Gilliland, D.; Garcìa, C. P.; Rossi, F. *J. Chromatogr., A* **2011**, *1218*, 4234−4239. (b) Schmidt, B.; Loeschner, K.; Hadrup, N.; Mortensen, A.; Sloth, J. J.; Koch, C. B.; Larsen, E. H. *Anal. Chem.* **2011**, *83*, 2461−2468. (c) Tsai, D. -H.; Cho, T. J.; DelRio, F. W.; Taurozzi, J.; Zachariah, M. R.; Hackley, V. A. *J. Am. Chem. Soc.* **2011**, *133*, 8884−8887.
(11) Novak, J. P.; Nickerson, C.; Franzen, S.; Feldheim, D. L. *Anal. Chem.* **2001**, *73*, 5758−5761.
(12) Akthakul, A.; Hochbaum, A. I.; Stellacci, F.; Mayes, A. M. *Adv. Mater.* **2005**, *17*, 532−535.
(13) McLeod, M. C.; Anand, M.; Kitchens, C. L; Roberts, C. B. *Nano Lett.* **2005**, *5*, 461−465.
(14) (a) Parak, W. J.; Pellegrino, T.; Micheel, C. M.; Gerion, D.; Williams, S. C.; Alivisatos, A. P. *Nano Lett.* **2003**, *3*, 33−36. (b) Negishi, Y.; Takasugi, Y.; Sato, S.; Yao, H.; Kimura, K.; Tsukuda, T. *J. Am. Chem. Soc.* **2004**, *126*, 6518−6519. (c) Zheng, M.; Huang, X. *J. Am. Chem. Soc.* **2004**, *126*, 12047−12054. (d) Negishi, Y.; Nobusada, K.; Tsukuda, T. *J. Am. Chem. Soc.* **2005**, *127*, 5261−5270. (e) Yao, J.; Miki, K.; Nishida, N.; Sasaki, A.; Kimura, K. *J. Am. Chem. Soc.* **2005**, *127*, 15536−15543. (f) Peterson, R. R.; Cliffel, D. E. *Anal. Chem.* **2005**, *77*, 4348−4353. (g) Gautier, C.; Bürgi, T. *J. Am. Chem. Soc.* **2006**, *128*, 11079−11087. (h) Hanauer, M.; Pierrat, S.; Zins, I.; Lotz, A.; Sönnichsen, C. *Nano Lett.* **2007**, *7*, 2881−2885. (i) Gautier, C.; Bürgi, T. *J. Am. Chem. Soc.* **2008**, *130*, 7077−7084. (j) Lo, C. K.; Paau, M. C.; Xiao, D.; Choi, M. M. F. *Anal. Chem.* **2008**, *80*, 2439−2446. (k) Yao, H.; Fukui, T.; Kimura, K. *J. Phys. Chem. C* **2008**, *112*, 16281−16285. (l) Kimura, K.; Sugimoto, N.; Sato, S.; Yao, H.; Negishi, Y.; Tsukuda, T. *J. Phys. Chem. C* **2009**, *113*, 14076−14082. (m) López-Lorente, A. I.; Simonet, B. M.; Valcárcel, M. *Trends Anal. Chem.* **2011**, *30*, 58−71. (n) Liu, F.-K. *Anal. Chim. Acta* **2011**, *694*, 167−173. (o) Levi-Kalisman, Y.; Jadzinsky, P. D.; Kalisman, N.; Tsunoyama, H.; Tsukuda, T.; Bushnell, D. A.; Kornberg, R. D. *J. Am. Chem. Soc.* **2011**, *133*, 2976−2982.
(15) Chak, C.-P.; Xuan, S.; Mendes, P. M.; Yu, J. C.; Cheng, C. H. K.; Leung, K. C.-F. *ACS Nano* **2009**, *3*, 2129−2138.
(16) Williams, D. P.; Satherley, J. *Langmuir* **2009**, *25*, 3743−3747.
(17) (a) Bai, L.; Ma, X.; Liu, J.; Sun, X.; Zhao, D.; Evans, D. G. *J. Am. Chem. Soc.* **2010**, *132*, 2333−2337. (b) Planken, K. L.; Cölfen, H. *Nanoscale* **2010**, *2*, 1849−1869. (c) Carney, R. P.; Kim, J. Y.; Qian, H.; Jin, R.; Mehenni, H.; Stellacci, F.; Bakr, O. M. *Nat. Commun.* **2011**, *2*, 335.
(18) (a) Wei, G.-T.; Liu, F.-K.; Wang, C. R. C. *Anal. Chem.* **1999**, *71*, 2085−2091. (b) Song, Y.; Jimenez, V.; McKinney, C.; Donkers, R.; Murray, R. W. *Anal. Chem.* **2003**, *75*, 5088−5096. (c) Jimenez, V. L.; Leopold, M. C.; Mazzitelli, C.; Jorgenson, J. W.; Murray, R. W. *Anal. Chem.* **2003**, *75*, 199−206. (d) Song, Y.; Heien, M. L.; Jimenez, V.; Wightman, R. M.; Murray, R. W. *Anal. Chem.* **2004**, *76*, 4911−4919. (e) Al-Somali, A. M.; Krueger, K. M.; Falkner, J. C.; Colvin, V. L. *Anal. Chem.* **2004**, *76*, 5903−5910. (f) Krueger, K. M.; Al-Somali, A. M.; Falkner, J. C.; Colvin, V. L. *Anal. Chem.* **2005**, *77*, 3511−3515. (g) Choi, M. M. F.; Douglas, A. D.; Murray, R. W. *Anal. Chem.* **2006**, *78*, 2779−2785. (h) Gies, A. P.; Hercules, D. M.; Gerdon, A. E.; Cliffel, D. E. *J. Am. Chem. Soc.* **2007**, *129*, 1095−1104. (i) Zhang, Y.; Shuang, S.; Dong, C.; Lo, C. K.; Paau, M. C.; Choi, M. M. F. *Anal. Chem.* **2009**, *81*, 1676−1685. (j) Arita, T.; Yoshimura, T.; Adschiri, T. *Nanoscale* **2010**, *2*, 167−1473. (k) Wu, Z.; MacDonald, M. A.; Chen, J.; Zhang, P.; Jin, R. *J. Am. Chem. Soc.* **2011**, *133*, 9670−9673.
(19) Murray, C. B.; Norris, D. J.; Bawendi, M. G. *J. Am. Chem. Soc.* **1993**, *115*, 8706−8715.
(20) Taleb, A.; Petit, C.; Pileni, M. P. *Chem. Mater.* **1997**, *9*, 950−959.
(21) (a) Lee, J. S.; Stoeva, S. I.; Mirkin, C. A. *J. Am. Chem. Soc.* **2006**, *128*, 8899−8903. (b) Wang, C.-L.; Fang, M.; Xu, S.-H.; Cui, Y.-P. *Langmuir* **2010**, *26*, 633−638. (c) Zhao, W.; Lin, L.; Hsing, I.-M. *Langmuir* **2010**, *26*, 7405−7409.
(22) (a) Whetten, R. L.; Khoury, J. T.; Alvarez, M. M.; Murthy, S.; Vezmar, I.; Wang, Z. L.; Stephens, P. W.; Cleveland, C. L.; Luedtke, W. D.; Landman, U. *Adv. Mater.* **1996**, *8*, 428−433. (b) Tracy, J. B.; Kalyuzhny, G.; Crowe, M. C.; Balasubramanian, R.; Choi, J. P.; Murray, R. W. *J. Am. Chem. Soc.* **2007**, *129*, 6706−6707.
(23) (a) Dass, A.; Stevenson, A.; Dubay, G. R.; Tracy, J. B.; Murray, R. W. *J. Am. Chem. Soc.* **2008**, *130*, 5940−5946. (b) Dass, A.; Guo, R.; Tracy, J. B.; Balasubramanian, R.; Douglas, A. D.; Murray, R. W. *Langmuir* **2008**, *24*, 310−315. (c) Dass, A.; Dubay, G. R.; Fields-Zinna, C. A.; Murray, R. W. *Anal. Chem.* **2008**, *80*, 6845−6849.
(24) Schaaff, T. G. *Anal. Chem.* **2004**, *76*, 6187−6196.
(25) (a) Dharmaratne, A. C.; Krick, T.; Dass, A. *J. Am. Chem. Soc.* **2009**, *131*, 13604−13605. (b) Dass, A. *J. Am. Chem. Soc.* **2009**, *131*, 11666−11667. (c) Knoppe, S.; Boudon, J.; Dolamic, I.; Dass, A.; Bürgi, T. *Anal. Chem.* **2011**, *83*, 5056−5061.
(26) Navin, J. K.; Grass, M. E.; Somorjai, G. A.; Marsh, A. L. *Anal. Chem.* **2009**, *81*, 6295−6299.
(27) (a) Harkness, K. M.; Fenn, L. S.; Cliffel, D. E; McLean, J. A. *Anal. Chem.* **2010**, *82*, 3061−3066. (b) Harkness, K. M.; Hixson, B. C.; Fenn, L. S.; Turner, B. N.; Rape, A. C.; Simpson, C. A.; Huffman, B. J.; Okoli, T. C.; McLean, J. A.; Cliffel, D. E *Anal. Chem.* **2010**, *82*, 9268−9274. (c) Harkness, K. M.; Cliffel, D. E.; McLean, J. A. *Analyst* **2010**, *135*, 868−874.
(28) Hostetler, M. J.; Wingate, J. E.; Zhong, C.-J.; Harris, J. E.; Vachet, R. W.; Clark, M. R.; Londono, J. D.; Green, S. J.; Stokes, J. J.; Wignall, G. D.; Glish, G. L.; Porter, M. D.; Evans, N. D.; Murray, R. W. *Langmuir* **1998**, *14*, 17−30.
(29) (a) Chen, S.; Ingram, R. S.; Hostetler, M. J.; Pietron, J. J.; Murray, R. W.; Schaaff, T. G.; Khoury, J. T.; Alvarez, M. M.; Whetten, R. L. *Science* **1998**, *280*, 2098−2101. (b) Lee, D.; Donkers, R. L.; Wang, G.; Harper, A. S.; Murray, R. W. *J. Am. Chem. Soc.* **2004**, *126*, 6193−6199.
(30) Chen, W.; Chen, S. *Angew. Chem., Int. Ed.* **2009**, *48*, 4386−4389.
(31) (a) Hakkinen, H.; Barnett, R. N.; Landman, U. *Phys. Rev. Lett.* **1999**, *82*, 3264−3267. (b) Chaki, N. K.; Negishi, Y.; Tsunoyama, H.; Shichibu, Y.; Tsukuda, T. *J. Am. Chem. Soc.* **2008**, *130*, 8608−8610.
(32) Look, J. L.; Zukoski, C. F. *J. Colloid Interface Sci.* **1992**, *153*, 469−482.